Interaction with a Biomolecule Facilitates the Formation of the Function-Determining Long-Lived Triplet State in a Ruthenium Complex for Photodynamic Therapy

Avinash Chettri[1,2], Houston D. Cole[3], John A. Roque III[3,4], Kilian R. A. Schneider[1,2], Tingxiang Yang[1,2], Colin G. Cameron[3], Sherri A. McFarland*[3], Benjamin Dietzek-Ivanšić*[1,2]

[1]Leibniz Institute of Photonic Technology Jena, Department Functional Interfaces, Albert-Einstein-Straße 9, 07745 Jena, Germany

[2]Friedrich Schiller University Jena, Institute of Physical Chemistry and Abbe Center of Photonics, Helmholtzweg 4, 07743 Jena, Germany

[3]The University of Texas at Arlington, Department of Chemistry and Biochemistry, Arlington, TX 76019, USA

[4]The University of North Carolina at Greensboro, Department of Chemistry and Biochemistry, Greensboro, NC 27402, USA

Corresponding authors: sherri.mcfarland@uta.edu and benjamin.dietzek@leibniz-ipht.de

Keywords: TLD1433; photodynamic therapy; ct DNA; excited state relaxation; long-lived triplet states

ABSTRACT

TLD1433 is the first ruthenium (Ru)-based photodynamic therapy (PDT) agent to advance to clinical trials and is currently in a Phase II study for treating non-muscle bladder cancer with PDT. Herein, we present a photophysical study of TLD1433 and its derivative TLD1633 using complex, biologically relevant solvents to elucidate the excited state properties that are key for biological activity. The complexes incorporate an imidazo [4,5-*f*][1,10]phenanthroline (IP) ligand appended to α-ter- or quaterthiophene, respectively, where TLD1433 = $[Ru(4,4'\text{-dmb})_2(IP\text{-}3T)]Cl_2$ and TLD1633 = $[Ru(4,4'\text{-dmb})_2(IP\text{-}4T)]Cl_2$ (4,4′-dmb=4,4′-dimethyl-2,2′-bipyridine; 3T=α-terthiophene; 4T= α-quaterthiophene). Time-resolved transient absorption experiments demonstrate that the excited state dynamics of the complexes change upon interaction with biological macromolecules (e.g., DNA). In this case, the accessibility of the lowest energy T_1 state is increased at the expense of a higher-lying triplet intraligand charge transfer (^{3}ILCT) state. We attribute this behavior to the increased rigidity of the ligand framework upon binding to DNA, which prolongs the lifetime of the T_1 state. This lowest lying state is primarily responsible for O_2 sensitization and hence photoinduced cytotoxicity. Therefore, in order to gain a realistic picture of the excited-state kinetics that underlie the photoinduced function of the complexes, it is necessary to interrogate their photophysical dynamics in the presence of biological targets once they are known.

INTRODUCTION

Photodynamic therapy (PDT) uses light to activate an otherwise nontoxic prodrug in the presence of oxygen to selectively destroy tumors and tumor vasculature, and is even capable of inducing an antitumor immune response.[1–5] The PDT reaction that results in damage to biomolecular targets is mediated by reactive oxygen species (ROS) formed via electron (Type I) or energy (Type II) transfer pathways between an excited state photosensitizer (PS) and oxygen. Singlet oxygen ($^1O_2$) is thought to be the most important ROS for the PDT effect.

Photofrin was the first PS approved for PDT,[6] and most subsequent-generation PSs are based on tetrapyrrolic structures.[7] These systems generate cytotoxic $^1O_2$ from $^3\pi\pi^*$ excited states. There has been ongoing interest in using transition metal complexes as PSs for PDT in order to improve upon earlier PSs. The structural modularity of transition metal complexes makes it relatively straightforward to tune their chemical and photophysical properties. This has been particularly well-documented for Ru(II) polypyridyl complexes, where a variety of excited states can be accessed by combining the appropriate ligands around the metal[8–13]: metal-to-ligand charge transfer (MLCT), metal-centered (MC), intraligand (IL), intraligand charge transfer (ILCT), and ligand-to- ligand charge transfer (LLCT).

The photophysical properties of transition metal complexes are generally understood in the context of the archetype $[Ru(bpy)_3]^{2+}$ complex, whereby the excited state dynamics tend to be controlled by the lowest-energy ^{3}MLCT state.[14,15] Light absorption first populates singlet states that undergo rapid intersystem crossing to form the lowest-lying ^{3}MLCT state. This state decays with a lifetime of approximately 1 μs in deoxygenated fluid solution[16] and 200 ns in the presence of oxygen.[17] Much work has been done to extend the triplet lifetimes in these systems for applications that rely on charge separation,[18–25] and prolonged lifetimes are likewise advantageous

for enhancing $^1O_2$ quantum yields in the area of PS design for PDT. One strategy involves creating bichromophoric systems that spatially isolate a pendant π-expanded organic chromophore from the Ru(II) center.[18–25] The resulting Ru metal-organic dyads have additional excited states that are localized to the organic chromophore, including triplet intraligand (^{3}IL) states of significant $^3\pi\pi^*$ character. Such states often have long μs lifetimes owing to the reduced intersystem crossing (ISC) rates associated with organic triplets. The ^{3}IL states can thus prolong the lifetimes of ^{3}MLCT states if they are relatively close in energy. If the ^{3}IL energy is substantially lower, then the triplet lifetimes can be even longer and exhibit characteristics of pure $^3\pi\pi^*$ states.[22] Such states in Ru(II) dyads can increase the $^1O_2$ quantum yields from near 56% for $[Ru(bpy)_3]^{2+}$ to almost unity. We have a longstanding interest in exploiting such systems for PDT applications since the prolonged lifetimes and improved $^1O_2$ yields correlate with better photocytotoxicity.[26,27]

Studies of the fundamental photophysical properties these Ru PSs (and related metal complexes) for PDT necessarily begin with understanding the excited state dynamics in simple solvents. However, ultimately, we want to unravel these dynamics in the complex cellular environment where factors such as pH, ionic strength, and interactions with biomolecules and cellular targets come into play and may substantially alter the photophysical properties. We have begun to undertake these more complicated studies[28,29] in an effort to elucidate the mechanism of action of our TLD1433, which is the only Ru-based PS to advance to clinical trials.[30,31]

Previous studies on a similar complex, bearing an imidazo [4,5-*f*][1,10]phenanthroline (IP) ligand appended to a pyrenyl substituent at C2 indicate that deprotonation of the imidazo moiety significantly alters the excited-state dynamics compared to the neutral or protonated species. This behavior is likely related to an increase in the energy gap between ^{3}MLCT and ^{3}IL states upon deprotonation of the ligand.[28] We also found that intercalation of this complex into salmon sperm

(SS) DNA altered the excited state dynamics by increasing the rate of coplanarization (between the imidizo and pyrene groups) compared to water as solvent.[29]

Herein we probe the effects of biologically relevant environments on the photophysical dynamics of two Ru dyads that incorporate an IP ligand appended to α-terthiophene (3T) or α-quaterthiophene (4T). Both TLD1433 (**Ru-ip-3T**) and TLD1633 (**Ru-ip-4T**) contain two 4,4′-dimethyl-2,2′-bipyridine (4,4′-dmb) as coligands and chloride as the counter ion: [Ru(4,4′-dmb)$_2$(IP-3T)]Cl$_2$ and [Ru(4,4′-dmb)$_2$(IP-4T)]Cl$_2$ (Figure 1). These two compounds are exceptional in vitro PDT agents toward cancer cells as demonstrated previously with the SK-MEL-28 melanoma cell line. The additional thienyl ring significantly impacted the photocytotoxicity, decreasing the EC_{50} value from 1.9×10^{-4} μM for **Ru-ip-3T** to 2.8×10^{-9} μM for **Ru-ip-4T**.[30] Spectroscopic studies in simple organic solvents and water revealed a complex interplay between ^{3}MLCT and ^{3}ILCT states. The ^{3}ILCT state was localized on the oligothiophene chain and dominated the overall photophysics of the complexes.[32] In water the long-lived triplet states were predominantly formed by vibrational cooling of hot ^{3}ILCT states, while the initial excitation populates a mixture of ^{1}MLCT and ^{1}ILCT states.[33] With increasing oligothiophene chain length, the lifetime of this state was extended into the range of a few tens of μs.[32] This study probes the effect of DNA-binding (although DNA is not the suggested biological target) and SK-MEL-28 cellular lysates [30,34,35] on these dynamics to underscore the importance of considering nonspecific biomolecular interactions that may influence the electronics and/or conformation of PSs when assessing the relevant photophysical mechanism(s) for photocytotoxicity.

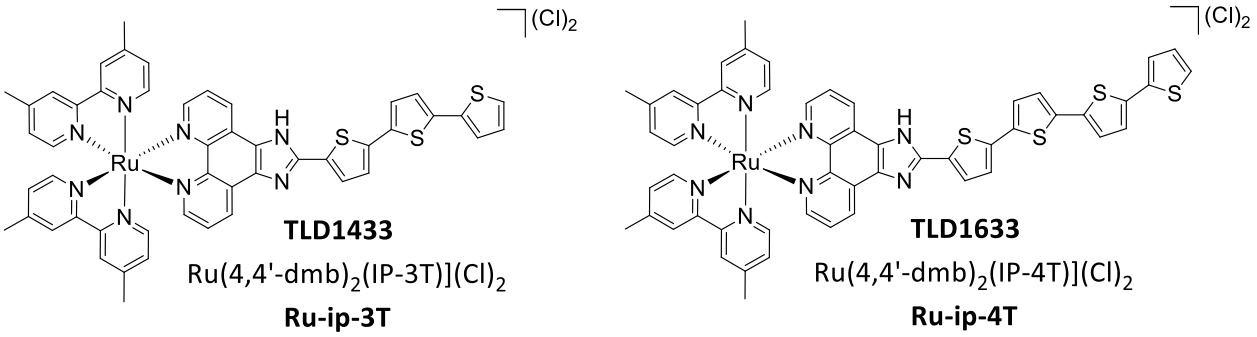

Figure 1. Chemical structures of (a) TLD1433, $[Ru(4,4'\text{-dmb})_2(IP\text{-}3T)]^{2+}$ (**Ru-ip-3T**) and (b) TLD1633, $[Ru(4,4'\text{-dmb})_2(IP\text{-}4T)]^{2+}$ (**Ru-ip-4T**). 4,4'-dmb=4,4'-dimethyl-2,2'-bipyridine; IP=imidazo [4,5-f][9,10] phenanthroline; 3T=α-terthiophene; 4T=α-quaterthiophene.

METHODS

ct DNA preparation. ct DNA was obtained from Sigma Aldrich (Merck) and reconstituted in Tris NaCl/HCl buffer (50 mM/5 mM, pH 7.4), sonicated, and frozen until further use. For all measurements in ct DNA, a fixed [DNA]bp / [complex] was used. The concentration of the ct DNA was determined from the UV−vis absorption signal of the ct DNA at 260 nm using OD = εcl, where εbp = 13 200 M^{-1} cm^{-1} (Figure S1).

Lysate preparation. Lysate was prepared from SK-MEL-28 cells at 90% confluence. The cells were detached using 5% trypsin-EDTA, pelleted with centrifugation, and then dissolved in PBS buffer commercially purchased from Merck (1X, without calcium and magnesium, pH 7.0-7.2) with several rounds of ultra-sonication at 30% power. Following sonication the concentrated lysate solution was diluted to 3 mL using Tris NaCl/HCl buffer (50 mM/5 mM, pH 7.4) and added to 50 μL of complex.

Steady state UV-vis absorption and emission spectroscopy. UV-vis absorption spectra were measured on a Jasco-V760 spectrophotometer in 1 cm quartz cell. Emission spectroscopy was carried out using a FLS980 spectrometer (Edinburgh Instruments) with a spectral resolution in the

excitation channel of $\Delta\lambda_{ex.}$=3 nm and $\Delta\lambda_{em.}$=4 nm in the emission channel. The OD of the sample was adjusted to 0.05 at the excitation wavelength for emission spectroscopy.

Time resolved spectroscopy. The setup for femtosecond time resolved spectroscopy in solution has been described elsewhere.[36,37] The maximum delay time window is 2 ns and the samples are excited at 400 nm using the second harmonic of the laser fundamental. Residual light from the fundamental was focused into a CaF_2 plate to generate the white light probe. The mutual polarization between pump and probe was set to the magic angle (54.7°). To avoid contributions from coherent artifacts[38,39] in the data analysis, data recorded at delay times shorter than 300 fs were omitted from the multi-exponential analysis.

For nanosecond transient absorption experiments, the 410 nm pump pulses are generated from an OPO pumped by the 10 Hz output of a NdYAG laser with a time resolution of 10 ns. The probe light is generated from an arc lamp, and the probe wavelength is stepped in 10 nm increments from 350 to 800 nm. The transient absorption signals are detected by a commercially available system from Princeton Instruments.

Samples. For ns-TA the OD at the excitation wavelength was set to 0.25 in a 1 cm quartz cell. The nanosecond transient absorption setup was also used for time-resolved emission measurements with the probe light blocked so that only the spontaneous emission was detected at 90° with respect to the pump beam. All experiments were carried out in duplicate.

For fs-TA measurements the OD of the sample in a 1 mm quartz cuvette was adjusted to 0.25 at the pump wavelength except for measurements in the presence of ct DNA where the OD was adjusted to 0.25 in a 1 cm quartz cell to achieve the desired $[DNA]_{bp}$/[complex] ratio. When

attempting to reach the desired high concentration of ct DNA in a 1 mm cell, precipitation of the DNA was observed. All experiments were performed in duplicate.

Data analysis procedure for femtosecond transient absorption. The transient absorption data was analyzed by fitting a kinetic model of the form:

$$\Delta A(\lambda, t) = \sum_1^i A_i e^{-t/\tau_i} + \text{Inf.}$$

In this analysis the probe-wavelength dependent coefficients A_i correspond to the decay-associated spectra (DAS), which are associated with specific characteristic first-order decay constants τ_i. Any component with a lifetime that exceeds the range of experimentally accessible delay times is summarized in the "Inf." spectrum in our fit. Thus, the corresponding DAS can be understood as the difference spectrum between the long-lived excited state and the ground state to which it relaxes.

RESULTS AND DISCUSSION

Steady state absorption and emission spectroscopy. The UV-vis absorption spectrum of **Ru-ip-3T** (Figure 2a) in water has two major transitions in the visible region, occuring at 420 and 480 nm. The former is assigned to ^{1}ILCT transitions while the latter corresponds to ^{1}MLCT transitions.[32] When **Ru-ip-3T** is mixed with ct DNA, these bands shift bathochromically by 5 nm (Figure 2a). Such spectral shifts are common for binding of Ru(II) complexes to ct DNA,[29,40] and similar shifts are observed for **Ru-ip-4T** (Figure S4). An earlier investigation we carried out on the related $[Ru(bpy)_2(IP\text{-}3T)]^{2+}$ complex with ct DNA showed a strong interaction characterized by a binding constant (K_b) on the order of ~10^8. Since the ionic strength and pH of buffer used in this study is identical to our previous study,[41] we anticipate similar K_b values for structurally similar complexes

such as $[Ru(dmb)_2(IP\text{-}3T)]^{2+}$ and $[Ru(bpy)_2(IP\text{-}3T)]^{2+}$. Upon interaction of these complexes with DNA, the long-wavelength absorption shoulder becomes more prominent which could prove convenient for inducing red-light activation of the complex for PDT.[42–44] Identical shifts are observed for **Ru-ip-3T** (Figure 2a) and **Ru-ip-4T** (Figure S6) in the presence of SK-MEL-28 lysate.

The weak ^{3}MLCT emission from both **Ru-ip-3T** and **Ru-ip-4T** is centered at 640 nm (upon excitation at 450 nm)[32] and does not shift in the presence of ct DNA. However, DNA enhances the emission by sixfold for **Ru-ip-3T** and by threefold for **Ru-ip-4T** (Figure 2b and Figure S4). This increased emission agrees with what has been previously observed for the structurally-related complex $[Ru(bpy)_2(IP\text{-}3T)]^{2+}$ bound to DNA[41] and has been attributed to the ability of DNA to shield the complex and thereby reduce excited state quenching by water or dissolved oxygen.[45,46] Unfortunately, large scattering effects precluded similar emission studies of **Ru-ip-3T** and **Ru-ip-4T** in SK-MEL-28 lysate solutions.

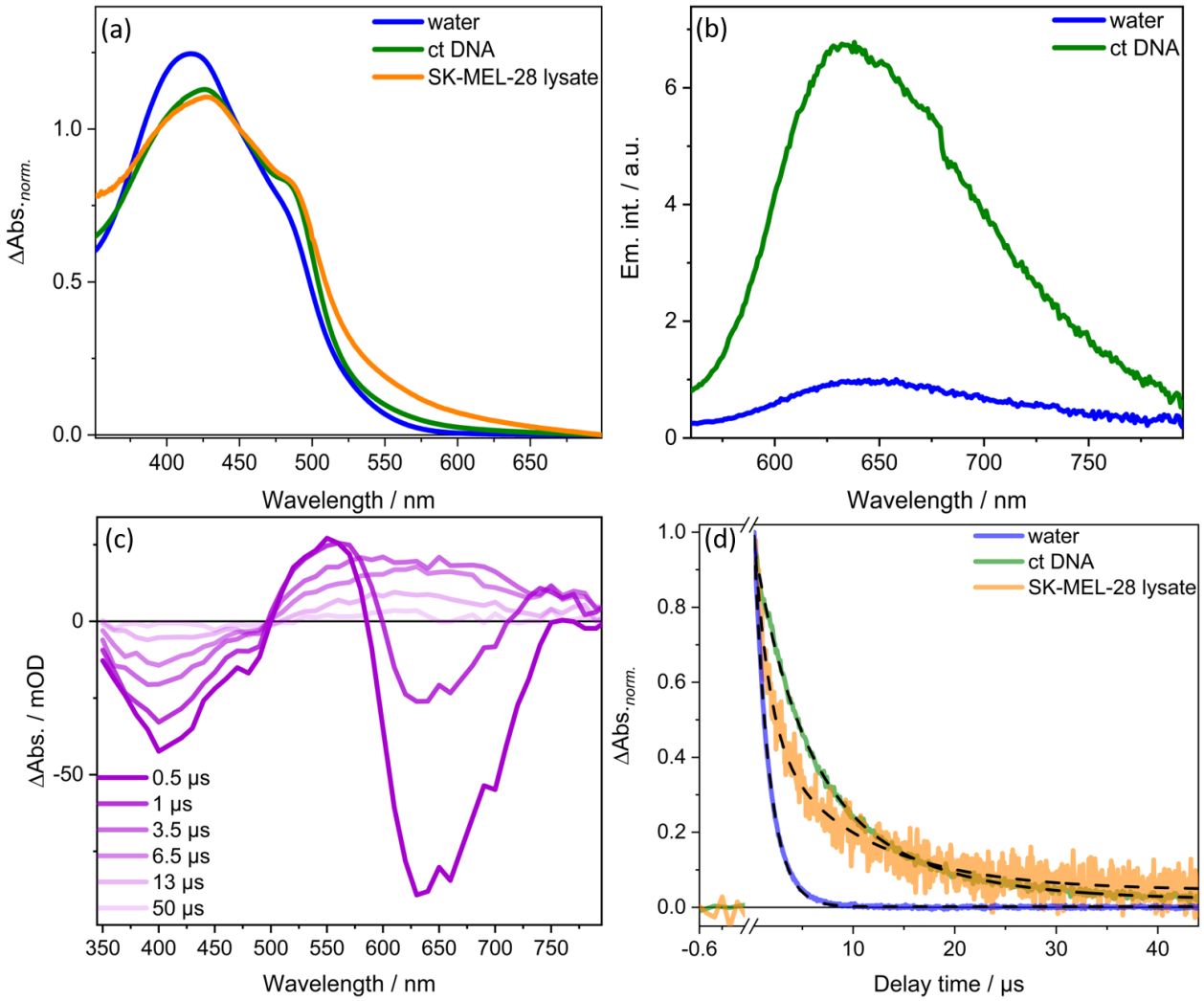

Figure 2. (a) Steady state UV-vis absorption spectra of **Ru-ip-3T** in water[32], ct DNA, and lysate of SK-MEL-28 cells. (b) Emission of **Ru-ip-3T** in water and ct DNA at excitation wavelength of 450 nm. (c) ns-TA of **Ru-ip-3T** in ct DNA recorded at selected delay times upon excitation at 410 nm. (d) Ground state recovery lifetimes (τ_{TA}) associated with T_1 state of **Ru-ip-3T** in water[32], ct DNA and lysates of SK-MEL-28 cell under aerated conditions. A $[DNA]_{bp}$/[complex] of 5:1 was used for all measurements in ct DNA solutions. Both ct DNA and SK-MEL-28 lysate solutions were prepared in Tris-HCl / NaCl (5 mM / 50 mM, pH 7.4) buffer. The kinetics from 630-680 nm were averaged to obtain the resultant kinetics and fitted to obtain the corresponding lifetimes. Note: For data analysis in Figure 2c, the contribution by emission is subtracted from the experimental data in the spectral range between 630 and 680 nm, thereby highlighting the features of the excited-state absorption spectrum (rather than the transient absorption spectrum, which of course contains information on emission). Experimentally, a transient absorption measurement is performed first. In order to account for the contribution by emission from this differential absorption kinetics, an additional measurement is conducted exclusively in only 'pump on' mode. This process allows us to separately collect the emission kinetics which is calibrated accordingly to ΔAbs. unit and subtracted from the differential absorption kinetics.

Nanosecond transient absorption and emission spectroscopy. As we previously reported,[32] the transient absorption (TA) spectrum obtained for **Ru-ip-3T** in water reveals an excited-state absorption (ESA) band at 640 nm, which was assigned to the lowest energy ^{3}ILCT state (referred to herein as the T_1 state)[32] that decays with a lifetime of 1.4 μs in aerated solution (Figure 2d). In addition to the T_1 decay, an emissive ^{3}MLCT state decays with a lifetime of 0.3 μs. The distinct lifetimes for T_1 and the ^{3}MLCT states indicate that they are not electronically coupled.

The nanosecond transient absorption spectra recorded for **Ru-ip-3T** in aqueous solution containing ct DNA solution show ESA features identical to those obtained in water. A broad ESA with a maximum at 640 nm represents absorption associated with the T_1 state, while a GSB occurs below 500 nm. The positive differential absorption band at 640 nm, reaching a maximum at 3.5 μs with a rise time constant of 0.5 μs (Figure 2c), results from overlap of the ESA with the ^{3}MLCT emission that yields a negative contribution to the differential absorption signal and decays on the sub-μs timescale. T_1 decays bi-exponentially with time constants of 4 (50%) and 10 μs (50%) as reflected in the ESA lifetime. The emissive ^{3}MLCT state for **Ru-ip-3T** in the presence of ct DNA also decays with a bi-exponential lifetime of 0.3 (60%) and 1.1 μs (40%) (Figure S2), with the shorter component being similar to the emissive lifetime in water. Bi-exponential emission kinetics suggests that there are two populations, a fraction of molecules that are unbound or loosely associated with ct DNA (the shorter component) alongside another that is more strongly bound (the longer component).

When **Ru-ip-3T** is dissolved in SK-MEL-28 cellular lysate, T_1 decays bi-exponentially with characteristic lifetimes of 1.4 (60%) and 10 μs (40%) (Figure 2d and Figure S2) observed by TA. The shorter time constant is consistent with that obtained in water, suggesting a population of

unbound or loosely-bound complexes in the lysate. It should be noted that there are a variety of biomolecules in the lysate, and thus multiple targets, but the observation of two lifetimes with roughly equal amplitudes suggests two major types of environments. Assuming that the shorter lifetime represents unbound or loosely-associated metal complex, we sought to use lysate not diluted with buffer in order to increase the concentration of DNA and other biomolecules in the solution. However, higher lysate concentrations led to immediate precipitation, precluding any determination on preferential lifetime effects.

We ascribe the increased stability of T_1, as reflected in the transient absorption data, to the fact that the biomolecule-bound complexes are less exposed to water and dissolved oxygen quenchers. A similar rational was used to explain the increase in the T_1 lifetime in the presence of ct DNA. The ^{3}MLCT lifetime of **Ru-ip-3T** is also prolonged by the lysate, increasing from 0.3 μs in water[32] to 0.5 μs in lysate (Figure S2). While comparable changes in lifetimes are observed for the T_1 state of **Ru-ip-3T** in DNA and lysate solutions, the effect on the MLCT state in DNA (appearance of a 1.1 μs component) is significantly greater than in lysate (0.5 μs). This could be due to stronger binding interactions by **Ru-ip-3T** in ct DNA solution compared to lysate. However further investigation is required to verify this hypothesis.

The behavior of **Ru-ip-4T** with ct DNA and SK-MEL-28 lysate is quantitatively identical to that of **Ru-ip-3T** (Figure S5). A bi-exponential decay of 1.4 (50%) and 7.4 μs (50%) corresponding to lifetimes of T_1 state with ct DNA is observed compared to 1.4 μs in water.[32] Also a bi-exponential ^{3}MLCT emission decay, characterized by decay times of 0.1 μs (40%) and 0.9 μs (60%), is observed and is suggestive of two populations (unbound or loosely-associated and bound). The T_1 state of **Ru-ip-4T** shows a bi-exponential decay with lifetimes of 1.4 μs (45%) and 10 μs (55%) in lysate (Figure S6), also suggestive of two environments with the shorter component

representing free complex. The increased T_1 lifetime in ct DNA solution and lysate would be expected to enhance $^1O_2$ sensitization even under low O_2 tension, an important consideration for PDT as many cancer cells thrive under low oxygen tension.[29,47]

	Ru-ip-3T					Ru-ip-4T				
	τ_1 / ps	**τ_2 / ps**	**τ_3 / ps**	**τ_{TA} / µs**	**$\tau_{em.}$ / µs**	**τ_1 / ps**	**τ_2 / ps**	**τ_3 / ps**	**τ_{TA} / µs**	**$\tau_{em.}$ / µs**
Water*	0.6	4.4	920	1.4	0.3	0.7	9.6	970	1.4	0.3
ct DNA	1	4	500	4, 10	0.3, 1.1	1	8	520	1.4, 7.4	0.1, 0.9
SK-MEL-28 lysate	-	4	600	1.4, 10	0.5	n.d.	n.d.	n.d.	1.4, 10	0.4

Table 1. Time constants associated with **Ru-ip-3T** and **Ru-ip-4T** in solutions under aerated conditions. Time constants, τ_{TA} and $\tau_{em.}$ are associated with the lifetimes of T_1 and ^{3}MLCT state respectively. The two time constants for τ_{TA} and $\tau_{em.}$ are due to contributions from unbound (shorter time constant) and bound (longer time constant) forms of the complexes. *Time constants obtained in water in the picosecond[33] and the microsecond range[32] are obtained from our previous studies. n.d. : not determined.

Femtosecond transient absorption spectroscopy. The fs transient absorption data of **Ru-ip-3T** along with its excited-state relaxation model, which is derived from femtosecond transient absorption spectra and the DAS spectra obtained from fitting the data, is discussed in our previous study.[33] Here we focus on the ultrafast photoinduced relaxation of **Ru-ip-3T** in a solution of ct DNA. The femtosecond TA spectra of **Ru-ip-3T** in the presence of ct DNA are characterized by a ground state bleach (GSB) flanked by two regions of excited state absorption (ESA). The ESA includes a weak positive ΔOD signal, which may indicate the presence of a band below 370 nm,s and a strong and broad positive ΔOD band above 550 nm (Figure 3a). Within the first 2.5 ps after photoexcitation, the initial GSB at 480 nm decreases, a negative ΔOD band at 420 nm emerges, and the initially broad and mostly structureless ESA increases. Subsequently, the ESA band sharpens into a peak at 660 nm on a 150 ps timescale. After the build-up of the 660 nm band, the

overall signal decays (but not completely) to the ns transient absorption features previously described (Figure 3a).

The data are analyzed quantitatively by fitting a sum of exponentials to give the characteristic decay times: τ_1=1 ps, τ_2=4 ps, and τ_3=500 ps. A long-lived component is also observed, which corresponds to the transients in the ns experiments. We refer to this component as the "infinite component" in the context of the femtosecond transient absorption spectra.

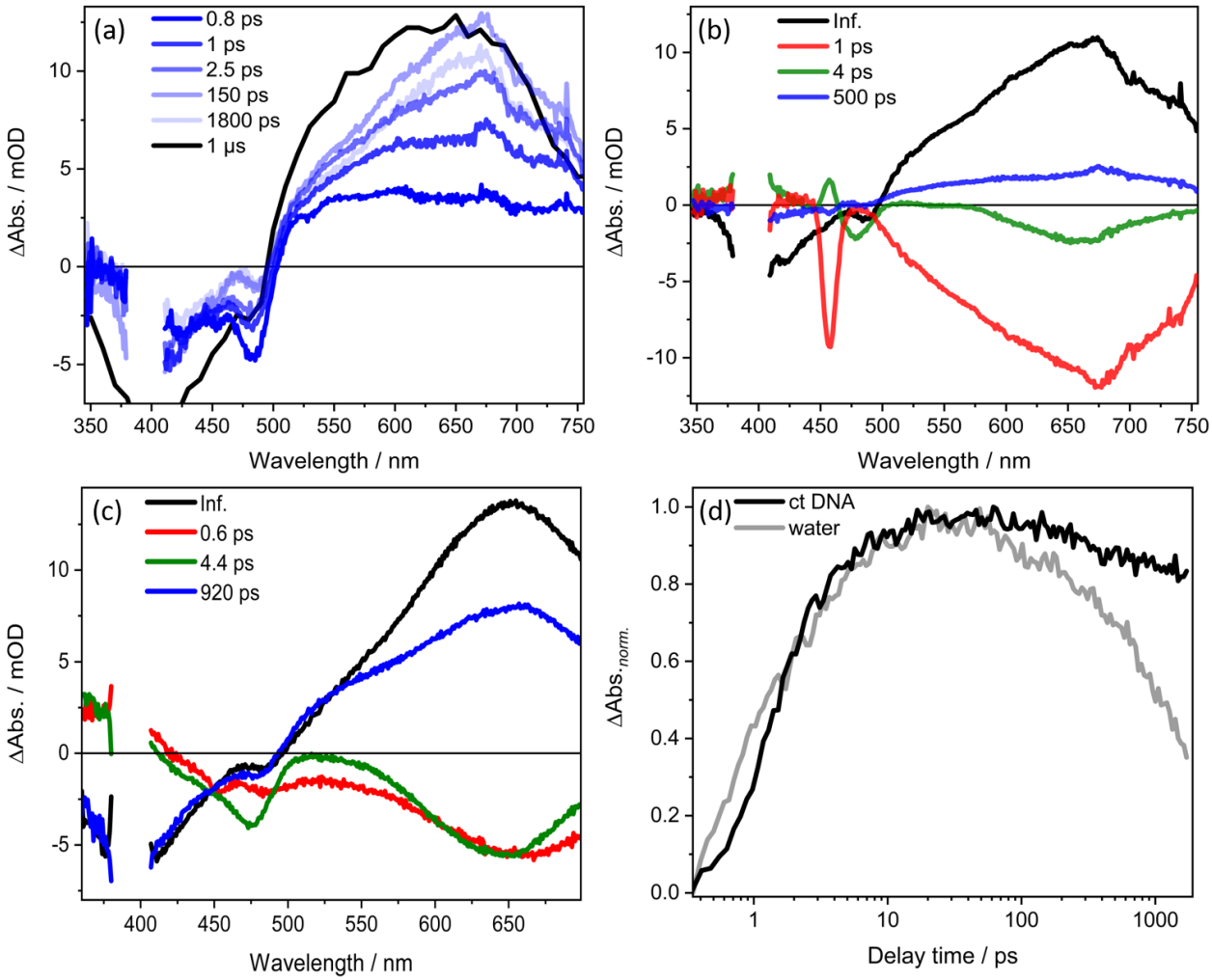

Figure 3. (a) Femtosecond TA spectra with 400-nm excitation of **Ru-ip-3T** in ct DNA solution. The spectrum at 1 µs is extracted from the ns-TA spectrum of **Ru-ip-3T** in ct DNA solution with contribution from emission subtracted from the overall spectra. (b) DAS for **Ru-ip-3T** in ct DNA solution. The intense band at at 460 nm in the 1-ps spectrum is due to Raman scattering by water. (c)

DAS for **Ru-ip-3T** in water. (d) Transient absorption kinetics recorded at 660 nm of **Ru-ip-3T** in ct DNA solution versus water following excitation at 400 nm. Data for **Ru-ip-3T** in water were reported elsewhere.[33]

The present data obtained in ct DNA solution (Figure 5) is interpreted in the context of the photophysical model derived for water as solvent, whereby photoexcitation leads to rapid ISC from the singlet to the triplet manifold that takes place within the temporal resolution of the experiment (120 fs).[14,15] The shortest relaxation time constant available from the data presented here, τ_1= 1 ps, is associated with hot ^{3}MLCT→^{3}ILCT energy transfer as indicated by a decrease in the MLCT bleach at 480 nm and an increase in the ILCT bleach at 420 nm with a simultaneous increase in the ESA band at 660 nm that is associated with the ^{3}ILCT state (Figure 3a). This is followed by the sharpening of the ESA at 660 nm with a time constant τ_2 = 4 ps. The process associated with τ_2 leads to a decrease in the ESA below 575 nm and above 700 nm (Figure 3b), with a simultaneous peaking of the band at 660 nm that is indicative of the molecules populating the lowest vibrational quanta of the ^{3}ILCT state. Hence, we associate this process to vibrational cooling from the initially populated hot ^{3}ILCT to form the cooled ^{3}ILCT state. The time constant of 500 ps (τ_3) decreases the overall ESA with a partial recovery of the GSB (Figure 3b). Though the DAS associated with the process is comparatively broader than the spectrum of the long-lived (infinite) component, it overall resembles the features of the ^{3}ILCT state. As discussed in our previous work,[33] this process is associated with the deactivation of molecules from a thermally-relaxed ^{3}ILCT state which has a molecular conformation different from the T_1 state.

Although the overall photophysical processes of **Ru-ip-3T** on a ps-timescale remain essentially unchanged upon binding to ct DNA, changes associated with τ_3 are observed. Interaction with ct DNA leads to a shorter characteristic time constant of 500 ps compared to 920 ps in water.[33] Furthermore, the contribution of the process (i.e., amplitude of the respective DAS) is smaller for the ct DNA solution. This can be rationalized by comparing the ratio *A* where

$$A = \frac{\text{Area}\left(\text{DAS}(\tau_{\text{Inf.}})\right)}{\text{Area}\left(\text{DAS}(\tau_3)\right)} \quad (1)$$

in the ct DNA solution (Figure 3b) with that in water (Figure 3c). In this equation, the area of $\tau_{Inf.}$ reflects the fraction of molecules populating the long lived T_1 state, while the area of τ_3 is proportional to the number of molecules decaying to the ground state from a higher lying ^{3}ILCT state.[33] In ct DNA solution, the ratio $A \approx 5$, whereas in water the value drops to 1.5. **Ru-ip-3T** strongly bound to ct DNA may orient the thiophene chain in conformation(s) favoring the population of T_1 over the cooled ^{3}ILCT state.

The femtosecond transient absorption profile of **Ru-ip-4T** bound to ct DNA (Figure 4a) also differs compared to **Ru-ip-4T** in water. As for **Ru-ip-3T** the relative weights of the processes associated with τ_3 and $\tau_{Inf.}$ change upon DNA binding (Figure 4). The lifetime associated with the decay of the cooled ^{3}ILCT state (τ_3) accelerates from 970 ps to 520 ps on moving from water to ct DNA solution. As for **Ru-ip-3T** the amplitude / contribution of this process to the overall signal is considerably lowered in ct DNA solution relative to water. We rationalize this by comparing the ratio *A* between ct DNA solution and water (4.5 versus 0.5, respectively), which implies that the population of the T_1 state dominates over the cooled ^{3}ILCT channel in ct DNA solution.

The ultrafast transient absorption data for **Ru-ip-4T** in ct DNA solution (Figure 4a) shows a GSB below 520 nm and an ESA at longer wavelengths. Within the first 15 ps, the GSB at 480 nm decreases with a simultaneous increase in the GSB at 425 nm. The ESA is marked by a peak at 700 nm and a broad shoulder at 550 nm. This ESA band which is primarily associated with a ^{3}ILCT state[33] increases within the first 15 ps. Following this delay time, the overall ESA signal decays with a concomitant decrease in the GSB. A sum of tri-exponential fit in addition to a long lived component (infinite) is used to globally fit the kinetics which yields the time constants: τ_1=1 ps,

τ_2=8 ps, and τ_3=520 ps (Figure 4b). The excited state model derived for **Ru-ip-4T** in water[33] can be used to account for its overall behavior in ct DNA solution. τ_1=1 ps increases the ESA at 700 nm which is associated with ^{3}ILCT state with a simultaneous decrease with the GSB at 480 nm. Hence, we associate this time constant with energy transfer from the hot ^{3}MLCT→hot ^{3}ILCT. τ_2=8 ps specifically results in a loss in ESA at 550 nm and 750 nm with an increase of the 700 nm peak, which represents the molecules relaxing to the lowest vibrational quanta of the ^{3}ILCT state. Therefore, the 8 ps time constant is associated with vibrational cooling from the hot ^{3}ILCT→cool ^{3}ILCT state. τ_3=520 ps leads to a decrease in the ESA and GSB. As mentioned above, we associate this process with a loss in the spectral features of the thermally relaxed ^{3}ILCT state (Figure 5), which is electronically and a conformationally distinct from the long-lived T_1 state.

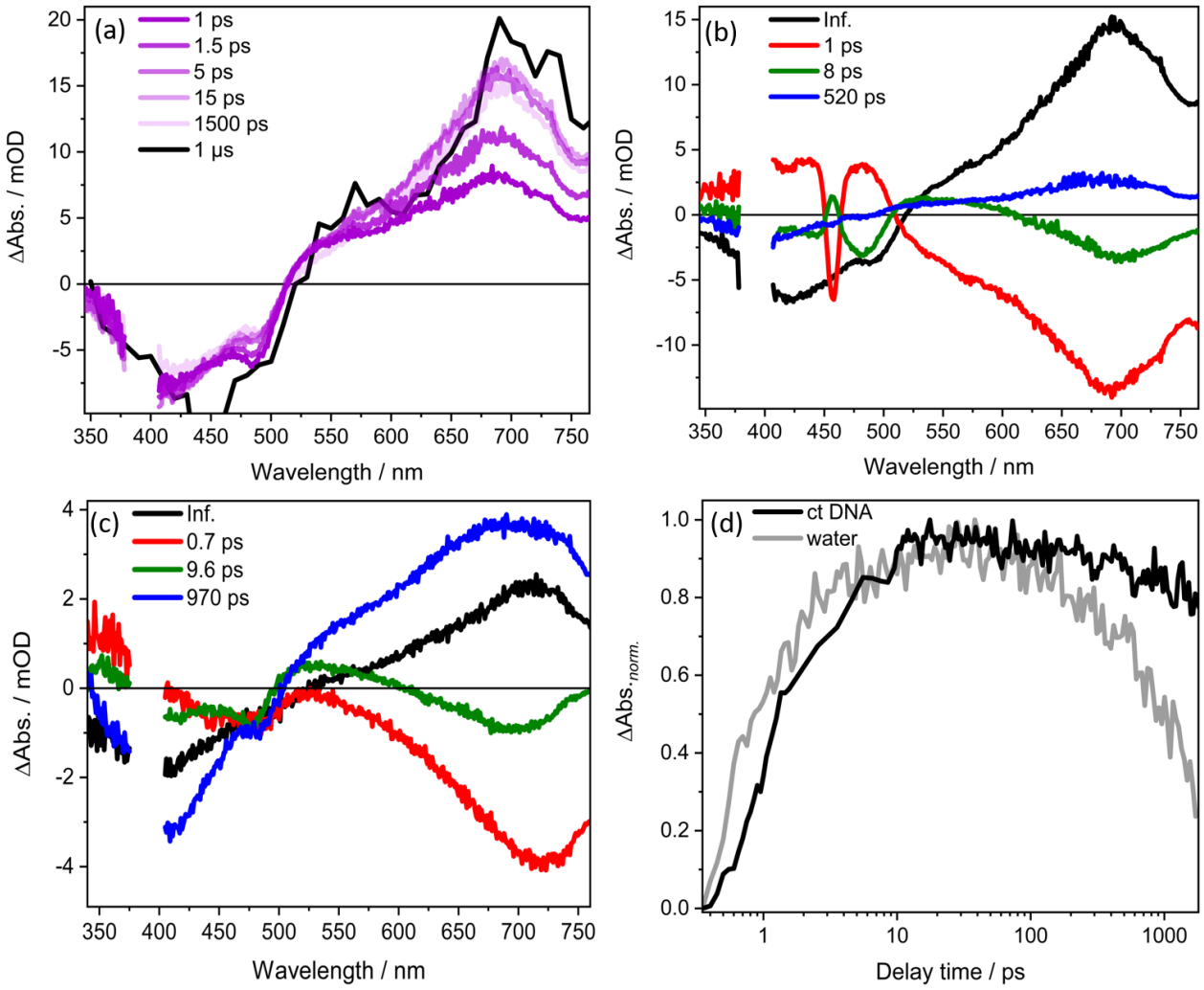

Figure 4. (a) Femtosecond TA spectra for **Ru-ip-4T** in ct DNA solution with 400-nm excitation. The spectrum at 1 µs is extracted from the ns-TA spectrum for **Ru-ip-4T** in ct-DNA solution with contribution from emission subtracted from the overall spectra. (b) DAS of **Ru-ip-4T** in ct DNA solution. The intense band at 460 nm in the 1-ps spectrum is due to Raman scattering by water. (c) DAS for **Ru-ip-4T** in water. (d) Transient absorption kinetics recorded at 700 nm of **Ru-ip-4T** in ct DNA solution versus water recorded upon excitation at 400 nm. Data for **Ru-ip-4T** in water was reported elsewhere.[33]

Our findings regarding the photoinduced dynamics in **Ru-ip-3T** and **Ru-ip-4T** when interacting with ct DNA indicate that increasing rigidity imposed on the complex may limit the number of conformations adopted, thereby affecting processes which are dependent on structural reorganization. This may selectively favor one excited-state relaxation pathway over the other.

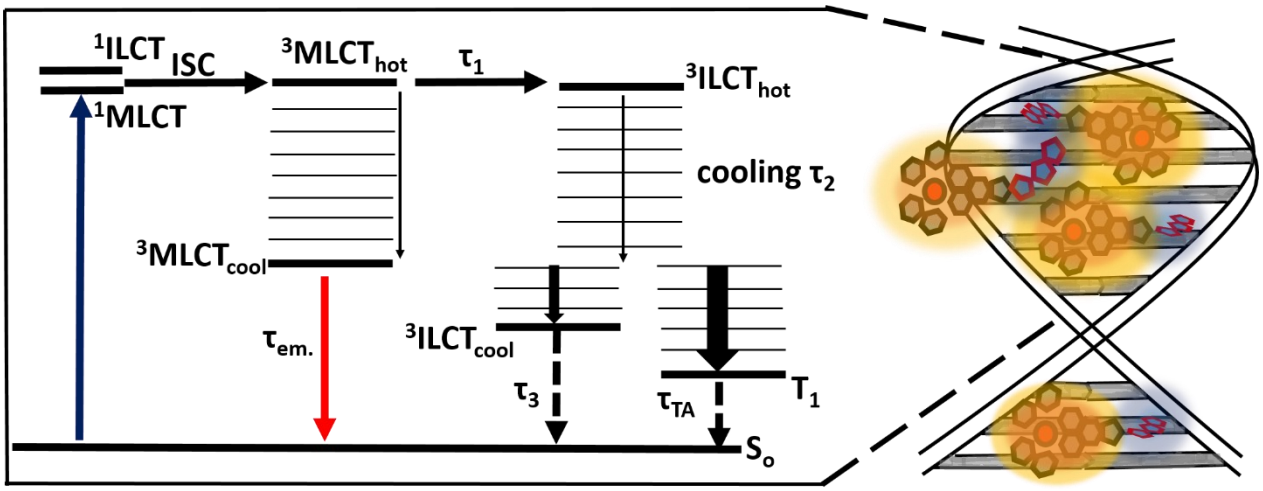

Figure 5. Jablonski diagram to describe the relaxation dynamics of **Ru-ip-3T** and **Ru-ip-4T** in biologically complex solvents with 400 nm excitation. The solid bold larger arrow in black indicates that the preferential population of T_1 state increases on moving from water to ct DNA solution. The ct DNA solution was 5:1 $[DNA]_{bp}$/[complex].

CONCLUSIONS

We investigated the excited state dynamics of the photoactive complex **Ru-ip-3T** in two representative biologically relevant environments, ct DNA and SK-MEL-28 cell lysate. We also explore the related **Ru-ip-4T** with ct DNA. Binding of the complexes to ct DNA alters their photoinduced dynamics compared to water as solvent. Most importantly, the decay of the oligothiophene-localized ^{3}ILCT state to reform the ground state was accelerated by interaction with the DNA, and the fraction of molecules that populate the long-lived T_1 state increases. Both findings hold true both for **Ru-ip-3T** and **Ru-ip-4T**. Thus, they indicate that also the excited-state reactivity in the triplet manifold, specifically the partitioning between the ^{3}ILCT and the T_1 state, is altered when the complexes interact with DNA. We tentatively ascribe this phenomenon to conformational restriction upon DNA binding, specifically with regard to the ip-*n*T ligand. Nanosecond transient absorption data show a significantly slower ground state recovery of the T_1 state when the complexes are in DNA or cell lysate solutions. The prolonged excited-state lifetime in the presence of biomolecules should enhance singlet oxygen production, an important

requirement for PDT. This study highlights the importance of interrogating the photophysical dynamics in solvents which are more biologically relevant than water in order to understand the function-determining excited-state processes in transition metal complexes designed to act as photoactive drugs.

ASSOCIATED CONTENTS

Supporting Information UV-visible spectra of ct DNA and SK-MEL-28 lysate for preparing solutions of requisite DNA concentration, nanosecond transient absorption spectra of **Ru-ip-3T** in SK-MEL-28 lysate and time resolved emission kinetics of **Ru-ip-3T** in SK-MEL-28 lysate and ct DNA with 410 nm excitation, femtosecond transient absorption spectra, DAS and kinetics of **Ru-ip-3T** in SK-MEL-28 lysate with 410 nm excitation, UV-visible absorption and emission spectra of **Ru-ip-4T** in buffer and ct DNA with 450 nm excitation, nanosecond transient absorption spectra, kinetics and time resolved emission kinetics of **Ru-ip-4T** in ct DNA with 410 nm excitation, UV-visible, nanosecond transient absorption spectra, kinetics and time resolved emission kinetics of **Ru-ip-4T** in SK-MEL-28 lysate with 410 nm excitation.

AUTHOR INFORMATION

Corresponding authors

Sherri A. McFarland- The University of Texas at Arlington, Department of Chemistry and Biochemistry, Arlington, TX 76019, USA. E mail: sherri.mcfarland@uta.edu

Benjamin Dietzek-Ivanšić- Leibniz-Institute of Photonic Technology Jena, Department Functional Interfaces, Albert-Einstein-Straße 9, 07745 Jena, Germany. E mail: benjamin.dietzek@leibniz-ipht.de

Friedrich-Schiller University Jena, Institute of Physical Chemistry, Helmholtzweg 4, 07743 Jena, Germany

Authors

Avinash Chettri- Leibniz-Institute of Photonic Technology Jena, Department Functional Interfaces, Albert-Einstein-Straße 9, 07745 Jena, Germany

Friedrich-Schiller University Jena, Institute of Physical Chemistry and Abbe Center of Photonics, Helmholtzweg 4, 07743 Jena, Germany; orcid.org/0000-0001-5500-5069

Kilian R.A. Schneider- Leibniz-Institute of Photonic Technology Jena, Department Functional Interfaces, Albert-Einstein-Straße 9, 07745 Jena, Germany

Friedrich-Schiller University Jena, Institute of Physical Chemistry, Helmholtzweg 4, 07743 Jena, Germany

Tingxiang Yang- Leibniz-Institute of Photonic Technology Jena, Department Functional Interfaces, Albert-Einstein-Straße 9, 07745 Jena, Germany

Friedrich-Schiller University Jena, Institute of Physical Chemistry, Helmholtzweg 4, 07743 Jena, Germany; orcid.org/0000-0003-4357-842X

Houston D. Cole- The University of Texas at Arlington, Department of Chemistry and Biochemistry, Arlington, TX 76019, USA

John A. Roque III- The University of Texas at Arlington, Department of Chemistry and Biochemistry, Arlington, TX 76019, USA

The University of North Carolina at Greensboro, Department of Chemistry and Biochemistry, Greensboro, NC 27402, USA

Colin G. Cameron- The University of Texas at Arlington, Department of Chemistry and Biochemistry, Arlington, TX 76019, USA

Notes

S.A.M. has a potential research conflict of interest due to a financial interest with Theralase Technologies, Inc. and PhotoDynamic, Inc. A management plan has been created to preserve objectivity in research in accordance with UTA policy

ACKNOWLEDGEMENTS

K.R.A.S. thanks the Carl-Zeiss-Foundation for financial support. A.C. and B.D.I. thank the DFG (project 395358570) for financial support.

S.A.M. and C.G.C. thank the National Science Foundation (NSF) (award 2102459) and the National Cancer Institute (NCI) of the National Institutes of Health (NIH) (Award R01CA222227) and the for partial support. The content in this review is solely the responsibility of the authors and does not necessarily represent the official views of the National Institutes of Health.

REFERENCES

(1) Bonnett, R. *Chemical Aspects of Photodynamic Therapy*; CRC Press: London, 2000.

(2) *Photodynamic Therapy: Basic Principles and Clinical Applications*; Henderson, B. W., Dougherty, T. J., Eds.; CRC Press: New York, 1992

(3) *Handbook of Photomedicine*, 1st ed.; Hamblin, M. R., Huang, Y., Eds.; CRC Press: Boca Raton, FL, 2013.

(4) Hamblin, M. R.; Mroz, P. *Advances in Photodynamic Therapy: Basic, Translational, and Clinical; Engineering in Medicine and Biology*; Artech House: Norwood, MA, 2008.

(5) *Photodynamic Medicine: From Bench to Clinic*, 1st ed.; Kostron, H., Hasan, T., Eds.; Royal Society of Chemistry: Cambridge, U.K., 2016.

(6) Usuda, J.; Kato, H.; Okunaka, T.; Furukawa, K.; Tsutsui, H.; Yamada, K.; Suga, Y.; Honda, H.; Nagatsuka, Y.; Ohira, T. Photodynamic Therapy (PDT) for Lung Cancers. *J. Thorac. Oncol.* **2006**, *1*, 489–493.

(7) Kataoka, H.; Nishie, H.; Hayashi, N.; Tanaka, M.; Nomoto, A.; Yano, S.; Joh, T. New Photodynamic Therapy with Next-Generation Photosensitizers. *Ann. Transl. Med.* **2017**, *5*, 183.

(8) Friedman, A. E.; Barton, J. K.; Chambron, J. C.; Sauvage, J. P.; Turro, N. J.; Barton, J. K. Molecular "Light Switch" for DNA: $Ru(bpy)_2(dppz)^{2+}$. *J. Am. Chem. Soc.* **1990**, *112*, 4960–4962.

(9) Howerton, B. S.; Heidary, D. K.; Glazer, E. C. Strained Ruthenium Complexes Are Potent Light-Activated Anticancer Agents. *J. Am. Chem. Soc.* **2012**, *134*, 8324–8327.

(10) Majewski, M. B.; Tacconi, N. R. D.; MacDonnell, F. M.; Wolf, M. O. Ligand-Triplet-Fueled Long-Lived Charge Separation in Ruthenium(II) Complexes with Bithienyl-Functionalized Ligands. *Inorg. Chem.* **2011**, *50*, 9939–9941.

(11) Sun, Y.; Joyce, L. E.; Dickson, N. M.; Turro, C. Efficient DNA Photocleavage by $[Ru(bpy)_2(dppn)]^{2+}$ with Visible Light. *Chem. Commun.* **2010**, *46*, 2426–2428.

(12) Hissler, M.; Harriman, A.; Khatyr, A.; Ziessel, R. Intramolecular Triplet Energy Transfer in Pyrene - Metal Polypyridine Dyads: A Strategy for Extending the Triplet Lifetime of the Metal Complex. *Chem. - A Eur. J.* **1999**, *5*, 3366–3381.

(13) Swavey, S.; Brewer, K. J. Visible Light Induced Photocleavage of DNA by a Mixed-Metal Supramolecular Complex: $[\{(bpy)_2Ru(dpp)\}_2RhCl_2]^{5+}$. *Inorg. Chem.* **2002**, *41*, 6196–6198.

(14) Bhasikuttan, A. C.; Suzuki, M.; Nakashima, S.; Okada, T. Ultrafast Fluorescence Detection in Tris(2,2′-bipyridine)ruthenium(II) Complex in Solution: Relaxation Dynamics Involving Higher Excited States. *J. Am. Chem. Soc.* **2002**, *124*, 8398–8405.

(15) Cannizzo, A.; Van Mourik, F.; Gawelda, W.; Zgrablic, G.; Bressler, C.; Chergui, M. Broadband Femtosecond Fluorescence Spectroscopy of $[Ru(bpy)_3]^{2+}$. *Angew. Chemie - Int. Ed.* **2006**, *45*, 3174–3176.

(16) Juris, A.; Balzani, V.; Barigelletti, F.; Campagna, S.; Belser, P.; von Zelewsky, A. Ru (II) Polypyridine Complexes: Photophysics, Photochemistry, Eletrochemistry, and

Chemiluminescence. *Coord. Chem. Rev.* **1988**, *84*, 85–277.

(17) Vögtle, F.; Plevoets, M.; Nieger, M.; Azzellini, G. C.; Credi, A.; De Cola, L.; De Marchis, V.; Venturi, M.; Balzani, V. Dendrimers with a Photoactive and Redox-Active $[Ru(bpy)_3]^{2+}$-Type Core: Photophysical Properties, Electrochemical Behavior, and Excited-State Electron-Transfer Reactions. *J. Am. Chem. Soc.* **1999**, *121*, 6290–6298.

(18) Ford, W. E.; Rodgers, M. A. J. Reversible Triplet-Triplet Energy Transfer within a Covalently Linked Bichromophoric Molecule. *J. Phys. Chem.* **1992**, *96* (7), 2917–2920.

(19) Goze, C.; Kozlov, D. V; Tyson, D. S.; Ziessel, R.; Castellano, F. N. Synthesis and Photophysics of Ruthenium (II) Complexes with Multiple Pyrenylethynylene Subunits. *New J. Chem.* **2003**, *27*, 1679–1683.

(20) Kozlov, D. V; Tyson, D. S.; Goze, C.; Ziessel, R.; Castellano, F. N. Room Temperature Phosphorescence from Ruthenium (II) Complexes Bearing Conjugated Pyrenylethynylene Subunits. *Inorg. Chem.* **2004**, *43*, 6083–6092.

(21) Tyson, D. S.; Henbest, K. B.; Bialecki, J.; Castellano, F. N. Excited State Processes in Ruthenium (II)/Pyrenyl Complexes Displaying Extended Lifetimes. *J. Phys. Chem. A* **2001**, *105*, 8154–8161.

(22) McClenaghan, N. D.; Leydet, Y.; Maubert, B.; Indelli, M. T.; Campagna, S. Excited-State Equilibration: A Process Leading to Long-Lived Metal-to-Ligand Charge Transfer Luminescence in Supramolecular Systems. *Coord. Chem. Rev.* **2005**, *249*, 1336–1350.

(23) Harriman, A.; Hissler, M.; Khatyr, A.; Ziessel, R. A Ruthenium (II) Tris (2,2′-bipyridine) Derivative Possessing a Triplet Lifetime of 42 μs. *Chem. Commun.* **1999**, 735–736.

(24) Simon, J. A.; Curry, S. L.; Schmehl, R. H.; Schatz, T. R.; Piotrowiak, P.; Jin, X.; Thummel, R. P. Intramolecular Electronic Energy Transfer in Ruthenium (II) Diimine Donor/Pyrene Acceptor Complexes Linked by a Single C− C Bond. *J. Am. Chem. Soc.* **1997**, *119*, 11012–11022.

(25) Harriman, A.; Khatyr, A.; Ziessel, R. Extending the Luminescence Lifetime of Ruthenium (II) Poly (Pyridine) Complexes in Solution at Ambient Temperature. *Dalt. Trans.* **2003**, 2061–2068.

(26) Monro, S.; Scott, J.; Chouai, A.; Lincoln, R.; Zong, R.; Thummel, R. P.; McFarland, S. A. Photobiological Activity of Ru (II) Dyads Based on (Pyren-1-yl) ethynyl Derivatives of 1, 10-Phenanthroline. *Inorg. Chem.* **2010**, *49* , 2889–2900.

(27) Lincoln, R.; Kohler, L.; Monro, S.; Yin, H.; Stephenson, M.; Zong, R.; Chouai, A.; Dorsey, C.; Hennigar, R.; Thummel, R. P. Exploitation of Long-Lived ^{3}IL Excited States for Metal–Organic Photodynamic Therapy: Verification in a Metastatic Melanoma Model. *J. Am. Chem. Soc.* **2013**, *135*, 17161–17175.

(28) Reichardt, C.; Sainuddin, T.; Wächtler, M.; Monro, S.; Kupfer, S.; Guthmuller, J.; Gräfe, S.; McFarland, S.; Dietzek, B. Influence of Protonation State on the Excited State Dynamics of a Photobiologically Active Ru(II) Dyad. *J. Phys. Chem. A* **2016**, *120*, 6379–6388.

(29) Reichardt, C.; Schneider, K. R. A.; Sainuddin, T.; Wächtler, M.; McFarland, S. A.; Dietzek, B. Excited State Dynamics of a Photobiologically Active Ru(II) Dyad Are Altered in Biologically Relevant Environments. *J. Phys. Chem. A* **2017**, *121*, 5635–5644.

(30) Monro, S.; Colón, K. L.; Yin, H.; Roque, J.; Konda, P.; Gujar, S.; Thummel, R. P.; Lilge,

L.; Cameron, C. G.; McFarland, S. A. Transition Metal Complexes and Photodynamic Therapy from a Tumor-Centered Approach: Challenges, Opportunities, and Highlights from the Development of TLD1433. *Chem. Rev.* **2019**, *119*, 797–828.

(31) McFarland, S. A.; Mandel, A.; Dumoulin-White, R.; Gasser, G. Metal-Based Photosensitizers for Photodynamic Therapy: The Future of Multimodal Oncology? *Curr. Opin. Chem. Biol.* **2020**, *56*, 23–27.

(32) Chettri, A.; Roque, J. A.; Schneider, K. R. A.; Cole, H. D.; Cameron, C. G.; McFarland, S. A.; Dietzek, B. It Takes Three to Tango: The Length of the Oligothiophene Chain Determines the Nature of the Long-Lived Excited State and the Resulting Photocytotoxicity of a Ruthenium(II) Photodrug. *ChemPhotoChem* **2021**, *5*, 421–425.

(33) Chettri, A.; Schneider, K. R. A.; Cole, H. D.; Roque III, J. A.; Cameron, C. G.; McFarland, S. A.; Dietzek, B. String-Attached Oligothiophene Substituents Determine the Fate of Excited States in Ruthenium Complexes for Photodynamic Therapy. *J. Phys. Chem. A* **2021**, *125*, 6985-6994.

(34) Lifshits, L. M.; Roque III, J. A.; Konda, P.; Monro, S.; Cole, H. D.; von Dohlen, D.; Kim, S.; Deep, G.; Thummel, R. P.; Cameron, C. G. et al. Near-Infrared Absorbing Ru(II) Complexes Act as Immunoprotective Photodynamic Therapy (PDT) Agents against Aggressive Melanoma . *Chem. Sci.* **2020**, *11*, 11740–11762.

(35) Roque, J. A.; Barrett, P. C.; Cole, H. D.; Lifshits, L. M.; Shi, G.; Monro, S.; Von Dohlen, D.; Kim, S.; Russo, N.; Deep, G. et al. Breaking the Barrier: An Osmium Photosensitizer with Unprecedented Hypoxic Phototoxicity for Real World Photodynamic Therapy. *Chem. Sci.* **2020**, *11*, 9784–9806.

(36) Karnahl, M.; Kuhnt, C.; Ma, F.; Yartsev, A.; Schmitt, M.; Dietzek, B.; Rau, S.; Popp, J. Tuning of Photocatalytic Hydrogen Production and Photoinduced Intramolecular Electron Transfer Rates by Regioselective Bridging Ligand Substitution. *ChemPhysChem* **2011**, *12* , 2101–2109.

(37) Siebert, R.; Akimov, D.; Schmitt, M.; Winter, A.; Schubert, U. S.; Dietzek, B.; Popp, J. Spectroscopic Investigation of the Ultrafast Photoinduced Dynamics in π-Conjugated Terpyridines. *ChemPhysChem* **2009**, *10*, 910–919.

(38) Kovalenko, S. A.; Dobryakov, A. L.; Ruthmann, J.; Ernsting, N. P. Femtosecond Spectroscopy of Condensed Phases with Chirped Supercontinuum Probing. *Phys. Rev. A - At. Mol. Opt. Phys.* **1999**, *59*, 2369–2384.

(39) Dietzek, B.; Pascher, T.; Sundström, V.; Yartsev, A. Appearance of Coherent Artifact Signals in Femtosecond Transient Absorption Spectroscopy in Dependence on Detector Design. *Laser Phys. Lett.* **2007**, *4*, 38–43.

(40) Sirajuddin, M.; Ali, S.; Badshah, A. Drug-DNA Interactions and Their Study by UV-Visible, Fluorescence Spectroscopies and Cyclic Voltametry. *J. Photochem. Photobiol. B Biol.* **2013**, *124*, 1–19.

(41) Shi, G.; Monro, S.; Hennigar, R.; Colpitts, J.; Fong, J.; Kasimova, K.; Yin, H.; DeCoste, R.; Spencer, C.; Chamberlain, L. et al. Ru(II) Dyads Derived from α-Oligothiophenes: A New Class of Potent and Versatile Photosensitizers for PDT. *Coord. Chem. Rev.* **2015**, *282–283*, 127–138.

(42) McKenzie, L. K.; Sazanovich, I. V.; Baggaley, E.; Bonneau, M.; Guerchais, V.; Williams, J. A. G.; Weinstein, J. A.; Bryant, H. E. Metal Complexes for Two-Photon Photodynamic

Therapy: A Cyclometallated Iridium Complex Induces Two-Photon Photosensitization of Cancer Cells under Near-IR Light. *Chem. - A Eur. J.* **2017**, *23*, 234–238.

(43) Al-Afyouni, M. H.; Rohrabaugh, T. N.; Al-Afyouni, K. F.; Turro, C. New Ru(II) Photocages Operative with near-IR Light: New Platform for Drug Delivery in the PDT Window. *Chem. Sci.* **2018**, *9*, 6711–6720.

(44) Zhang, P.; Wang, Y.; Qiu, K.; Zhao, Z.; Hu, R.; He, C.; Zhang, Q.; Chao, H. A NIR Phosphorescent Osmium(II) Complex as a Lysosome Tracking Reagent and Photodynamic Therapeutic Agent. *Chem. Commun.* **2017**, *53*, 12341–12344.

(45) Tan, L. F.; Wang, F.; Chao, H.; Zhou, Y. F.; Weng, C. Ruthenium(II) Mixed-Ligand Complex Containing 2-(4′-benzyloxy-phenyl)imidazo[4,5-f][1,10]phenanthroline: Synthesis, DNA-Binding and Photocleavage Studies. *J. Inorg. Biochem.* **2007**, *101* (4), 700–708.

(46) Wu, J. Z.; Yuan, L. Synthesis and DNA Interaction Studies of a Binuclear Ruthenium(II) Complex with 2,9-bis(2-imidazo[4,5-f][1,10]phenanthroline)-1,10-phenanthroline as Bridging and Intercalating Ligand. *J. Inorg. Biochem.* **2004**, *98*, 41–45.

(47) Reichardt, C.; Monro, S.; Sobotta, F. H.; Colón, K. L.; Sainuddin, T.; Stephenson, M.; Sampson, E.; Roque, J.; Yin, H.; Brendel, J. C. et al. Predictive Strength of Photophysical Measurements for in Vitro Photobiological Activity in a Series of Ru(II) Polypyridyl Complexes Derived from π-Extended Ligands. *Inorg. Chem.* **2019**, *58*, 3156–3166.

TOC GRAPHIC